Available online at www.sciencedirect.com
SCIENCE DIRECT®
Journal of Solid State Chemistry 179 (2006) 145–155
JOURNAL OF SOLID STATE CHEMISTRY
www.elsevier.com/locate/jssc

Inorganic–organic hybrid compounds: Synthesis and characterization of three new metal phosphonates with similar characteristic structural features

Sebastian Bauer[a], Thomas Bein[b], Norbert Stock[a,*]

[a]*Institute of Inorganic Chemistry, Christian-Albrechts-University, Otto-Hahn-Platz 6/7, D 24118 Kiel, Germany*
[b]*Department of Chemistry and Biochemistry, Ludwig-Maximilians-University, Butenandtstr. 5-13 (E), D 81377 Munich, Germany*

Received 11 August 2005; received in revised form 7 October 2005; accepted 9 October 2005
Available online 15 November 2005

Abstract

The phosphonocarboxylic acid $H(HO_3PCH_2)_2NH\text{-}CH_2C_6H_4\text{-}COOH$ (**H_5L**) was synthesized and characterized by NMR- and IR-spectroscopy, thermogravimetric (TG) analysis and single-crystal X-ray diffraction. Reactions of **H_5L** with samarium(III) chloride and calcium(II) chloride resulted in three new compounds, $Sm[(O_3PCH_2)_2NH\text{-}CH_2C_6H_4\text{-}COOH]\cdot H_2O$ (**1**), $Ca[H(O_3PCH_2)_2NH\text{-}CH_2C_6H_4\text{-}COOH]\cdot H_2O$ (**2**), and $Ca[(HO_3PCH_2)_2NH\text{-}CH_2C_6H_4\text{-}COOH]_2\cdot 4H_2O$ (**3**). The single-crystal structure determination of the title compounds reveals that in **H_5L** as well as in compounds **1**, **2**, and **3** zwitterions are present. Within the *M*–O building units of the metal phosphonates we observed a different degree of dimensionality, depending on the oxidation state of the metal ion and the synthesis conditions. In **1**, one-dimensional chains of edge-sharing SmO_8 polyhedra are observed while in **2**, isolated units of edge-sharing CaO_6 octahedra and in **3** isolated CaO_6 octahedra are observed. However, looking at the organic part, the rigid phenyl carboxylic acid moieties arrange in a ''zipper-like'' fashion and hydrogen bonding plays an important role in the stabilization of the crystal structure. The title compounds were further characterized by IR spectroscopy and TG analysis. Additionally, the thermal stability of **1** was investigated by temperature-dependent X-ray diffraction.

Keywords: Metal phosphonates; Phosphonocarboxylic acid; Inorganic–organic hybrid compounds; Crystal structure; Samarium; Calcium

1. Introduction

Hybrid materials with organic and inorganic moieties are an attractive field of research due to their composite properties and the possibility of tuning their chemistry [1]. The potential of these inorganic–organic hybrid materials lies in their use as sorbents, ion exchangers, catalysts, or charge storage materials. In the field of metal carboxylates a concept for the rational design of porous compounds has been developed that allows in some cases the systematical variation of the pore size and functionality [2]. In contrast, in metal phosphonate chemistry there seem to be left too many unknown factors for controlling the structure such as the high coordination flexibility of the phosphonate group. Nevertheless, metal phosphonates are promising candidates for the synthesis of inorganic–organic hybrid open-framework materials [3]. We are interested in the systematic investigation of polyphosphonic and phosphonocarboxylic acids as starting materials for the synthesis of new metal phosphonates. The goal is to establish structural and synthetic trends in these systems for a better understanding of metal phosphonate chemistry. Thus, we have established high-throughput methods in our group, which allow us the systematic and rapid investigation of reactions under hydrothermal conditions [4–7]. Recently, we have started an investigation in the application of functionalized iminobis (methylphosphonic acid)-derivatives, $(H_2O_3PCH_2)_2N\text{-}R$, for the synthesis of metal phosphonates [8,9]. Thus, by reacting $(H_2O_3PCH_2)_2$

*Corresponding author. Fax: +49 431 880 1775.
E-mail address: stock@ac.uni-kiel.de (N. Stock).

0022-4596/$ - see front matter © 2005 Elsevier Inc. All rights reserved.
doi:10.1016/j.jssc.2005.10.008

N-$(CH_2)_4$-N$(CH_2PO_3H)_2$ [6,10], and $(H_2O_3PCH_2)_2$N-$CH_2C_6H_4CH_2$-N$(CH_2PO_3H)_2$ [11] with different metal ions we obtained a number of new compounds, some containing three-dimensional framework structures and one showing reversible dehydration/hydration properties. For current studies, we chose the ligand $H(HO_3PCH_2)_2NH\text{-}CH_2C_6H_4$-COOH (**$H_5L$**) were the carboxylic acid group is separated from the bisphosphonic acid group by means of the phenyl group. This rigid moiety in combination with the flexible coordination properties of the iminobis (methylphosphonic acid) and carboxylic acid functionality makes H_5L a promising candidate for the synthesis of new metal phosphonates with interesting structural features. Since limited information on the chemistry of the ligand H_5L is available [9,12,13] high-throughput methodology is the method of choice to systematically study its coordination behavior in the presence of different metal ions. In one detailed study, we recently obtained four new cobalt compounds, $Co_2[(O_3PCH_2)_2N\text{-}CH_2C_6H_4\text{-}COOH]\cdot H_2O$, $Co[(O_3PCH_2)(OCH)N\text{-}CH_2C_6H_4\text{-}COOH]\cdot H_2O$, $Co[H_2(O_3PCH_2)_2N\text{-}CH_2C_6H_4\text{-}COOH]$, and $[Co_2(O_3PCH_2)_2N\text{-}CH_2C_6H_4\text{-}COOH]\cdot 3.5H_2O$ [9].

Since only structures of **H_5L** with Zn^{2+}, Co^{2+}, and Pb^{2+} are known [9,12,13], we were further interested in the chemistry of other two-valent cations and those with higher oxidation states. Herein, we report on the synthesis and characterization of three new metal phosphonates, $Sm[(O_3PCH_2)_2NH\text{-}CH_2C_6H_4\text{-}COOH]\cdot H_2O$ (**1**), $Ca[H(O_3PCH_2)_2NH\text{-}CH_2C_6H_4\text{-}COOH]\cdot H_2O$ (**2**), and $Ca[(HO_3PCH_2)_2NH\text{-}CH_2C_6H_4\text{-}COOH]_2\cdot 4H_2O$ (**3**). Furthermore, we were able to additionally characterize H_5L by single-crystal structure determination and compare the thermal behavior as well as the IR-spectroscopic properties of all four compounds.

2. Experimental section

2.1. Synthesis of $H(HO_3PCH_2)_2NH\text{-}CH_2C_6H_4\text{-}COOH$

The carboxyaryl-iminobis (methylphosphonic acid), was synthesized by a Mannich-type reaction starting from 4-(aminomethyl)benzoic acid, phosphoric acid, and formaldehyde [9,14].

2.2. Synthesis of $Sm[(O_3PCH_2)_2NH\text{-}CH_2C_6H_4\text{-}COOH]\cdot H_2O$ (1)

$Sm[(O_3PCH_2)_2NH\text{-}CH_2C_6H_4\text{-}COOH]\cdot H_2O$ (**1**) was prepared by reacting 53.8 mg (159 μmol) H_5L, 120 μL (120 μmol) of a 1 M aqueous solution of $SmCl_3\cdot 6H_2O$, and 130 μL deionized water in a sealed 500 μL Teflon microreactor. The reaction was carried out at 150 °C for 4 days. The resulting single-phase yellow product was filtered and washed with deionized water and acetone. X-ray powder diffraction experiments confirmed the presence of only one phase, $Sm[(O_3PCH_2)_2NH\text{-}CH_2C_6H_4COOH]\cdot H_2O$ (**1**). In order to investigate the influence of the molar ratio Sm:H_5L and the influence of the pH of the starting mixture, reactions with different molar ratios xSm:$y$$H_5L$:$z$NaOH (see Supplementary Material) were performed in a 48-reactor multiclave [6,15]. After the work-up and characterization by automated X-ray powder diffraction all products were identified as microcrystalline $Sm[(O_3PCH_2)_2NH\text{-}CH_2C_6H_4\text{-}COOH]\cdot H_2O$. No additional phase was observed.

2.3. Synthesis of $Ca[H(O_3PCH_2)_2NH\text{-}CH_2C_6H_4\text{-}COOH]\cdot H_2O$ (2)

In a reaction of 19 mg (56 μmol) H_5L with 28 μL 2 M aqueous $CaCl_2\cdot 2H_2O$ solution (56 μmol), 66 μL 2.5 M aqueous NaOH solution (165 μmol), and 156 μL $\cdot H_2O$ in a Teflon microreactor at 150 °C for four days, single crystals of $Ca[H(O_3PCH_2)_2NH\text{-}CH_2C_6H_4\text{-}COOH]\cdot H_2O$ (**2**) among pure phase microcrystalline product were obtained. This was confirmed by X-ray powder diffraction measurements.

2.4. Synthesis of $Ca[(HO_3PCH_2)_2NH\text{-}CH_2C_6H_4\text{-}COOH]_2\cdot 4H_2O$ (3)

To investigate the influence of the temperature on the product formation in the system Ca^{2+}:H_5L:NaOH:H_2O the following reaction was performed. 75.0 mg (0.221 mmol) H_5L were dispersed in 3 mL $\cdot H_2O$ in a supersonic bath. The dispersion was heated to 100 °C. After the addition of a solution of 21.7 mg (0.148 mmol) $CaCl_2\cdot 2H_2O$ in 2 mL $\cdot H_2O$ a colorless solid precipitates. The suspension is again heated to 100 °C and treated in the supersonic bath. The sample was allowed to cool to room temperature. Over night needles of colorless single-crystals of $Ca[(HO_3PCH_2)_2NH\text{-}CH_2C_6H_4\text{-}COOH]_2\cdot 4H_2O$ formed over microcrystalline product. Both products were shown to be identical by X-ray powder diffraction measurement.

2.5. Physical characterization

High-throughput X-ray analysis was carried out using a STOE high-throughput powder diffractometer equipped with an image-plate detector system [6]. The data collection time was 6 min per sample. High-precision X-ray powder diffraction patterns were recorded with a STOE STADI P diffractometer using monochromated Cu$K\alpha_1$ radiation. IR spectra were recorded on a Bruker IFS 66v/S FTIR spectrometer in the spectral range 4000–400 cm^{-1} using the KBr disk method. Thermogravimetric (TG) analyses were carried out in air (25 mL/min, 30-900 °C, 10 °C/min) using a NETZSCH STA 449C Analyzer (compounds **1** and **2**) or a NETZSCH STA 429 Analyzer (compound **3**).

3. Crystallography

The single-crystal structure determination by X-ray diffraction for $H(HO_3PCH_2)_2NH\text{-}CH_2C_6H_4\text{-}COOH$ (**H_5L**),

compounds **1**, and **2** was performed on a STOE IPDS diffractometer equipped with a fine-focus sealed-tube X-ray source (Mo$K\alpha$ radiation, $\lambda = 0.71073$ Å) operating at 55 kV and 50 mA. For data reduction and the absorption correction the program Xred was used [16]. For compound **3**, the data collection was performed on a STOE Imaging Plate Diffraction System (IPDS-1). All single-crystal structures were solved by direct methods and refined using the program package SHELXTL [17]. All H-atoms bound to carbon atoms were placed onto calculated positions. These H-atoms were refined using a riding model and fixing the temperature factor to be 1.2 times the value of the atom they are bonded to. Additionally, for H-atoms bound to O-atoms that could be located from the difference Fourier maps the O–H bond distance was set to 0.82 Å H-atoms bound to N-atoms that could be located from the difference Fourier maps the N–H bond distance was set to 0.86 Å. These atoms were refined using a riding model and fixing the temperature factor to be 1.5 (in case of oxygen) or 1.2 (in case of nitrogen) times the value of the atom they are bonded to. The crystal data for $H(HO_3PCH_2)_2NH\text{-}CH_2C_6H_4\text{-}COOH$ and compounds **1**–**3** is listed in Table 1. Selected bond distances and hydrogen bonds are given in Tables 2–5 and Tables S2–S5 in the Supplementary Material, respectively.

4. Results and discussion

4.1. Crystal structures

4.1.1. Crystal structure of $H(HO_3PCH_2)_2NH\text{-}CH_2C_6H_4\text{-}COOH$

The asymmetric unit of the phosphonocarboxylic acid is shown in Fig. S1 in the Supplementary Material and selected bond lengths are given in Table 2. The three-dimensional structure is composed of $H(HO_3PCH_2)_2NH\text{-}CH_2C_6H_4\text{-}COOH$ zwitterions, in which one phosphonic acid group is monodeprotonated and the N-atom is protonated (Fig. S1). The positions of the hydrogen atoms were unambiguously derived from the single-crystal structure determination. The N-atom and all O-atoms except the carbonyl oxygen O8 are involved in a hydrogen bonding scheme in such way as to stabilize the structure (Table S2 in the Supplementary Material). In Fig. 1, the H-bonding modes of the dihydrogen-phosphonate group (P1) are given. Oxygen atoms O2 and O3 interact as H-donor

Table 1
Summary of crystal data, intensity measurement, and structure refinement parameters for $H(HO_3PCH_2)_2NH\text{-}CH_2C_6H_4\text{-}COOH$ (H_5L), $Sm((O_3PCH_2)_2NH\text{-}CH_2C_6H_4\text{-}COOH)\cdot H_2O$ (**1**), $Ca(H(O_3PCH_2)_2NH\text{-}CH_2C_6H_4\text{-}COOH)\cdot H_2O$ (**2**), and $Ca((HO_3PCH_2)_2NH\text{-}CH_2C_6H_4\text{-}COOH)_2\cdot 4H_2O$ (**3**)

Compound	H_5L	1	2	3
Crystal system	Monoclinic	Orthorhombic	Monoclinic	Monoclinic
Space group	$P2_1/c$	$Pbca$	$P2_1/n$	$P2_1/c$
a (pm)	5.5953(1)	6.9890(3)	5.7132(3)	17.056(1)
b (pm)	34.0036(6)	32.925(2)	7.9600(4)	7.4224(4)
c (pm)	7.0121(1)	12.9079(7)	31.729(2)	14.018(1)
α (deg)	90	90	90	90
β (deg)	94.8644(7)	90	94.396(7)	114.164(8)
γ (deg)	90	90	90	90
Volume (10^6 pm^3)	1329.32(4)	2970.3(3)	1438.7(1)	1619.2(2)
Z	4	8	4	2
Formula mass (g/mol)	339.17	504.51	395.25	788.47
ρ (g/cm^3)	1.69	2.256	1.825	1.617
F (000)	704	1960	816	820
Crystal size (mm^3)	$0.11\times0.08\times0.06$	$0.15\times0.07\times0.03$	$0.43\times0.05\times0.03$	$0.1\times0.02\times0.02$
μ (mm^{-1})	0.368	4.217	0.708	0.478
Absorption correction	Numerical	Numerical	Numerical	Numerical
T_{min}/T_{max}	0.9595/0.9796	0.6930/0.880	0.9505/0.9866	0.9595/0.9796
θ range (deg)	3.134–27.485	2.0–28.0	2.58–27.97	2.62–25.08
Range in hkl	$-7\leqslant h\leqslant 7$, $-43\leqslant k\leqslant 43$, $-9\leqslant l\leqslant 9$	$-8\leqslant h\leqslant 9$, $-43\leqslant k\leqslant 21$, $-16\leqslant l\leqslant 17$	$-7\leqslant h\leqslant 6$ $-10\leqslant k\leqslant 10$ $-41\leqslant l\leqslant 41$	$-18\leqslant h\leqslant 18$ $-7\leqslant k\leqslant 8$, $-16\leqslant l\leqslant 16$
Total data collect.	18207	13224	12109	7174
Unique/obs. data ($I>2\sigma(I)$)	3029/2192	3471/2090	3369/2433	2475/2192
Extinction coeff.	None	None	None	0.013(2)
R(int)	0.0863	0.0790	0.0645	0.0572
$R1$, w$R2$ ($I>2\sigma(I)$)	0.0412, 0.0984	0.0342, 0.0557	0.0331, 0.0694	0.0364/0.0804
$R1$, w$R2$ (all data)	0.0708, 0.1121	0.0740, 0.0621	0.0525, 0.0734	0.0572/0.0874
Goodness of fit	1.025	0.824	0.895	0.965
No. of variables	250	209	209	216
Δe min/max (eÅ^{-3})	−0.516/0.511	−0.969/0.882	−0.393/0.460	−0.319/0.310

Table 2
Selected bond distances (Å) for $H(HO_3PCH_2)_2NH\text{-}CH_2C_6H_4\text{-}COOH$

P1–O1	1.482 (2)	P2–O4	1.497 (2)
P1–O2	1.533(2)	P2–O5	1.509 (2)
P1–O3	1.563(2)	P2–O6	1.564(2)
P1–C1	1.813(2)	P2–C2	1.819(3)
C–N	1.502(3)–1.524(3)	C3–C4	1.501(3)
$C–C_{phenyl}$	1.379(4)–1.397(4)	C7–C10	1.483(3)
C10–O8	1.215(3)	C10–O7	1.336(3)

Table 3
Selected bond distances (Å) for $Sm[(O_3PCH_2)_2NH\text{-}CH_2C_6H_4\text{-}COOH]\cdot H_2O$ (**1**)

Sm–O	2.319(4)–2.649(4)	P–C	1.845(6)–1.828(7)
P1–O1	1.521(4)	P2–O4	1.519(4)
P1–O2	1.523(5)	P2–O5	1.539(4)
P1–O3	1.539(4)	P2–O6	1.501(3)
C–N	1.512(7)–1.517(7)	C3–C4	1.497(9)
$C–C_{phenyl}$	1.37 (1)–1.408(9)	C7–C10	1.478(10)
C10–O7	1.329(8)	C10–O8	1.217(7)

Table 4
Selected bond distances (Å) for $Ca(H(O_3PCH_2)_2NH\text{-}CH_2C_6H_4\text{-}COOH)\cdot H_2O$ (**2**)

Ca–O	2.303 (2)–2.442 (2)	P–C	1.836(2)–1.834(2)
P1–O1	1.488 (2)	P2–O4	1.534 (2)
P1–O2	1.510(2)	P2–O5	1.505 (2)
P1–O3	1.562 (2)	P2–O6	1.527(2)
N–C	1.501(3)–1.519(3)	C3–C4	1.507(3)
$C–C_{phenyl}$	1.384(4)–1.393(3)	C7–C10	1.500(3)
O7–C10	1.317(3)	O8–C10	1.199(3)

Table 5
Selected bond distances (Å) and angles (deg) for $Ca((HO_3PCH_2)NH\text{-}CH_2C_6H_4\text{-}COOH)_2\cdot 4H_2O$

Ca–O	2.280(2)–2.384(2)	P–C	1.827(3)–1.828(3)
P1–O1	1.488(2)	P2–O4	1.571(2)
P1–O2	1.512(2)	P2–O5	1.486(2)
P1–O3	1.567(2)	P2–O6	1.512(2)
C–N	1.516(4)–1.528(4)	C3–C4	1.512(4)
$C–C_{phenyl}$	1.386(5)–1.397(5)	C7–C10	1.498(4)
O7–C10	1.323(4)	O8–C10	1.214(4)

atoms with O6 and O4 (O2-H···O6:2.477(2) Å; O3-H···O4: 2.597(2) Å) of two different monohydrogenphosphonate groups (P2). The oxygen O1 is a twofold H-acceptor, interacting with N1-H and O8-H from the carboxylic acid group (N1-H···O1: 2.792(2) Å; O8-H···O1: 2.854(2) Å). The H-bonding modes of the monohydrogenphosphonate group (P2) are shown in Fig. 2. Only oxygen O5 is protonated and by employing oxygen O4 and O5, the phosphonate groups (P2) form a hydrogen bonding pattern (O5-H···O4: 2.591(2) Å) well-known from carboxylic acid

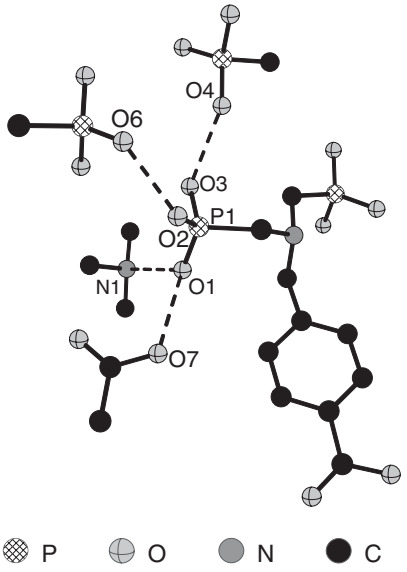

Fig. 1. H-bonding modes of the phosphonate group P1 in $H(HO_3PCH_2)_2NH\text{-}CH_2C_6H_4\text{-}COOH$.

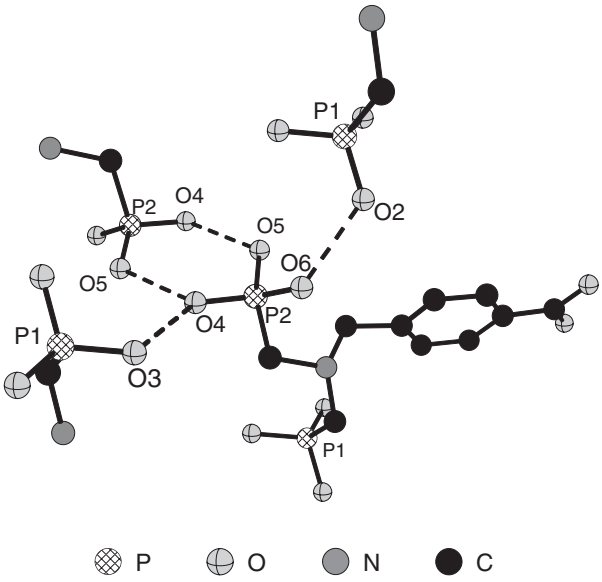

Fig. 2. H-bonding modes of the phosphonate group P2 in $H(HO_3PCH_2)_2NH\text{-}CH_2C_6H_4\text{-}COOH$.

dimers. These different kinds of H-bonding schemes result in a structure that can be described as hydrogen-phosphonate layers in the *a*,*c*-plane (Fig. 3) that are zipper-like interconnected via H-bonding of aryl-carboxylic acid groups (Fig. 4). The different H-bonds are well reflected in the P–O and C–O bond distances obtained from the crystal structure determination.

*4.1.2. Crystal structure of $Sm[(O_3PCH_2)_2NH\text{-}CH_2C_6H_4\text{-}COOH]\cdot H_2O$ (**1**)*

The asymmetric unit of $Sm[(O_3PCH_2)_2NH\text{-}CH_2C_6H_4COOH]\cdot H_2O$ is shown in Fig. S2. It consists of one Sm^{3+}

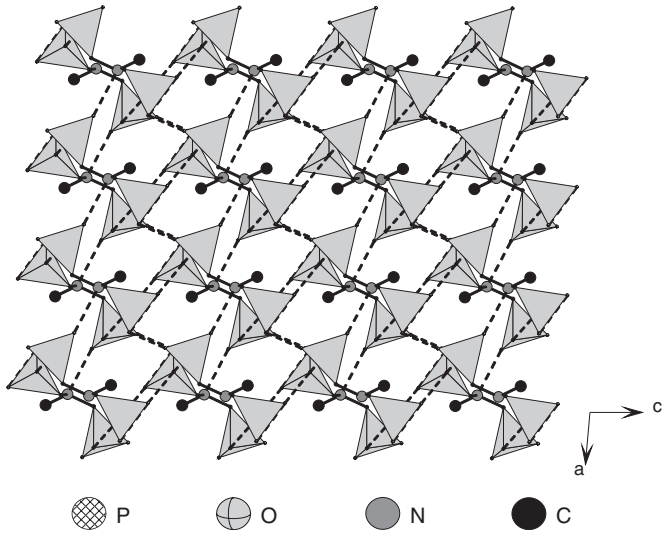

Fig. 3. Hydrogen-phosphonate layer in the *a*,*c*-plane as observed in $H(HO_3PCH_2)_2NH\text{-}CH_2C_6H_4\text{-}COOH$. The gray tetrahedra describe the PCO_3-group.

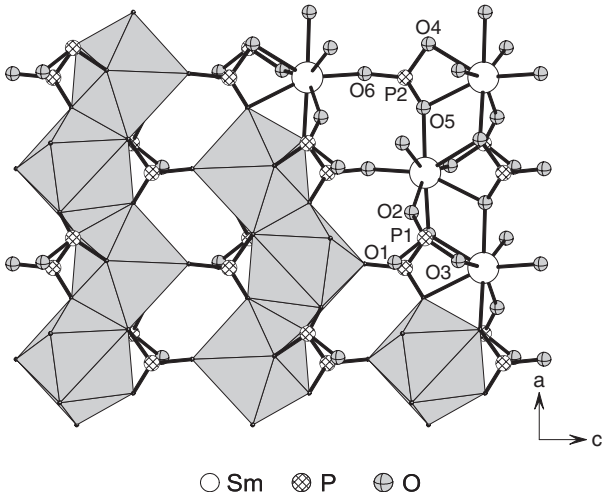

Fig. 5. Chains of SmO_8-polyhedra are connected via phosphonate groups to form a samarium phosphonate layer parallel to the *a*,*c*-plane as observed in $Sm[(O_3PCH_2)_2NH\text{-}CH_2C_6H_4\text{-}COOH]\cdot H_2O$ (**1**). The SmO_8-polyhedra are presented in light gray.

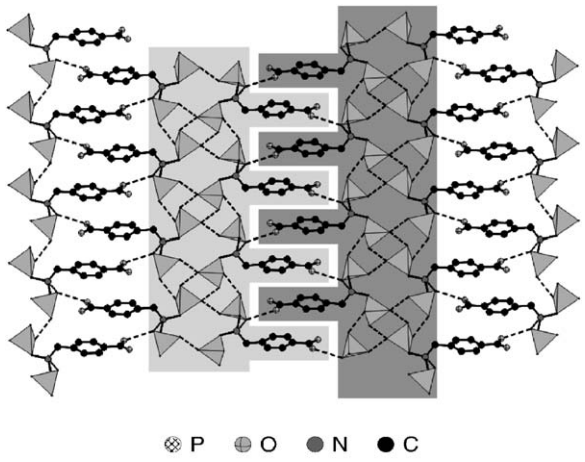

Fig. 4. Zipper-like interconnection of the hydrogen phosphonate layers via aryl-carboxylic acid groups in $H(HO_3PCH_2)_2NH\text{-}CH_2C_6H_4\text{-}COOH$. The gray tetrahedra describe the PCO_3-group.

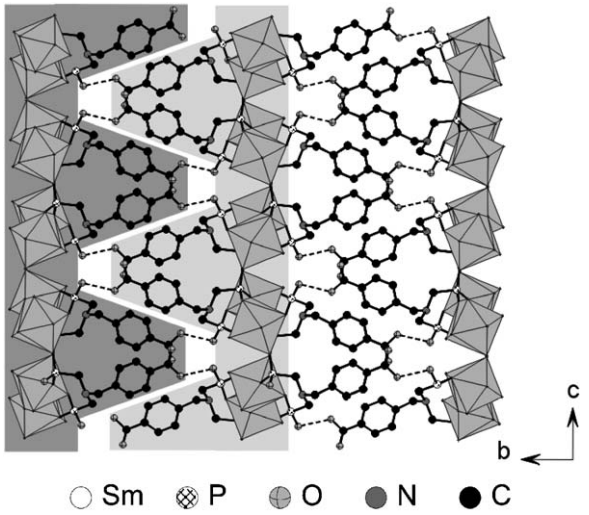

Fig. 6. Zipper-like interconnection of adjacent samarium phosphonate layers by hydrogen bonding (dashed lines) between carboxylic acid and phosphonate groups in $Sm[(O_3PCH_2)_2NH\text{-}CH_2C_6H_4\text{-}COOH]\cdot H_2O$ (**1**). The SmO_8-polyhedra are presented in light gray.

ion, one $[(O_3PCH_2)_2NH\text{-}CH_2C_6H_4COOH]^{3-}$ zwitterion, and one water molecule. The hydrogen atom bonded to nitrogen and one hydrogen atom bonded to the water molecule (O9) could be located from difference Fourier maps. The samarium ions are coordinated by seven oxygen atoms belonging to phosphonate groups and the water molecule. Edge-sharing SmO_8-polyhedra form chains along the *a*-axis that are further stabilized by the phosphonate group (Fig. 5). The phosphonic acid groups are fully deprotonated and all phosphonate oxygens except oxygen O1 are involved in the coordination of the metal centers. Whereas the oxygen atoms O2 and O3 of the phosphonate group around P1 are each bound to only one samarium ion, the phosphonate group around P2 acts as a chelating ligand through oxygen O4 and O5 and at the same time these oxygen atoms bridge to adjacent samarium ions (μ_2 oxygen). The interconnection of these chains is accomplished through the coordination of an oxygen atom (O6) to a samarium ion of an adjacent chain (Fig. 5). The organic units are arranged in a zipper-like fashion with the carboxylic acid groups pointing to neighboring layers (Fig. 6). Thus, hydrogen bonds between the carboxylic acid group (O7-H) and the oxygen atom O1 of the phosphonate group P1 of a adjacent layer are formed. The proton of the carboxylic acid group could not be located from the difference Fourier map. However, the bond distances in the carboxylic acid group (C10-O7: 1.329(8) Å, C10-O8: 1.217(7) Å) strongly suggest that oxygen O7 is protonated and acts as proton donor in the hydrogen bonding scheme O7H···O1 (Table S3). The short interatomic distance (2.547 Å) implies a strong hydrogen bond [18]. The

structure is further stabilized via extensive N–H···O and O–H···O hydrogen bonding (Fig. S3 in the Supplementary Material).

4.1.3. Crystal structure of $Ca[H(O_3PCH_2)_2NH\text{-}CH_2C_6H_4\text{-}COOH]\cdot H_2O$ (2)

The asymmetric unit of **2** consists of one Ca^{2+} ion, one $[H(O_3PCH_2)_2NH\text{-}CH_2C_6H_4\text{-}COOH]^{2-}$ zwitterion, and one water molecule (Fig. S4). All positions of the hydrogen atoms were unambiguously derived from the difference Fourier map. The Ca^{2+} ion are octahedrally surrounded by five oxygen atoms of the phosphonate and one water molecule. Two edge-sharing CaO_6 octahedra connect to form centrosymmetric Ca_2O_{10} units (Fig. 7). The coordination behavior of the organic unit is given in Fig. 8. Two oxygen atoms of each phosphonate group are involved in the coordination of Ca^{2+} ions. Oxygens O1, O2, and O5 are only binding to a single Ca^{2+} ion, whereas oxygen O4 acts as a μ_2 ligand bridging two Ca^{2+} ions of the Ca_2O_{10} units. Thus, Ca_2O_{10} units are connected by phosphonate groups to form Ca-phosphonate layers in the *a*,*b*-plane (Fig. 9). These layers are stabilized by extensive N–H···O and O–H···O hydrogen bonding (Fig. S5 and Table S4 in the Supplementary Material). The organic units point into the interlayer space with the carboxylic acid groups directed to the adjacent layers. Thus, a zipper-like connection of neighboring layers stabilized by hydrogen bonding between the carboxylic acid oxygen O7 and phosphonate oxygen O6 is observed (Fig. 10). This theme is very similar to that observed in the structures of $H(HO_3P)_2NH\text{-}CH_2C_6H_4\text{-}COOH$ and $Sm[(O_3PCH_2)_2NH\text{-}CH_2C_6H_4\text{-}COOH]\cdot H_2O$.

4.1.4. Crystal structure of $Ca[(HO_3PCH_2)_2NH\text{-}CH_2C_6H_4\text{-}COOH]_2\cdot 4H_2O$ (3)

The asymmetric unit of **3** is given in Fig. S6. It is comprised of one $[(HO_3PCH_2)_2NH\text{-}CH_2C_6H_4\text{-}COOH]^-$

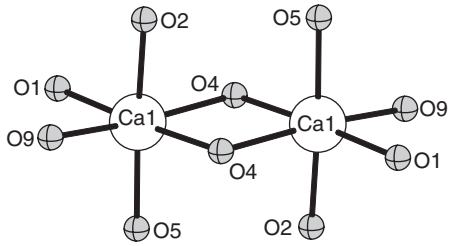

Fig. 7. Two edge-sharing CaO_6 octahedra form centrosymmetric Ca_2O_{10} units, as observed in $Ca[H(O_3PCH_2)_2NH\text{-}CH_2C_6H_4\text{-}COOH]\cdot H_2O$ (**2**).

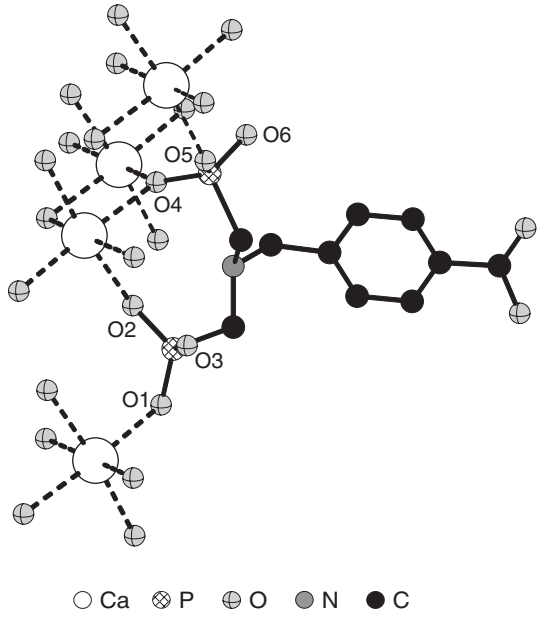

Fig. 8. Coordination behavior of the organic unit in $Ca[H(O_3PCH_2)_2NH\text{-}CH_2C_6H_4\text{-}COOH]\cdot H_2O$ (**2**).

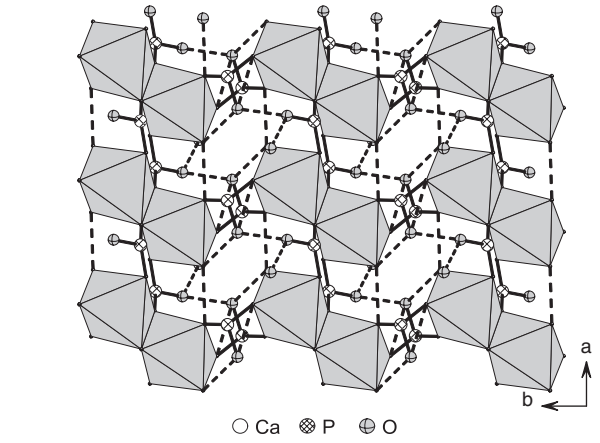

Fig. 9. In $Ca[H(O_3PCH_2)_2NH\text{-}CH_2C_6H_4\text{-}COOH]\cdot H_2O$ (**2**), the Ca_2O_{10} units are connected via phosphonate groups to form Ca-phosphonate layers in the *a*,*b*-plane. The layers are further stabilized by hydrogen bonding (dashed lines).

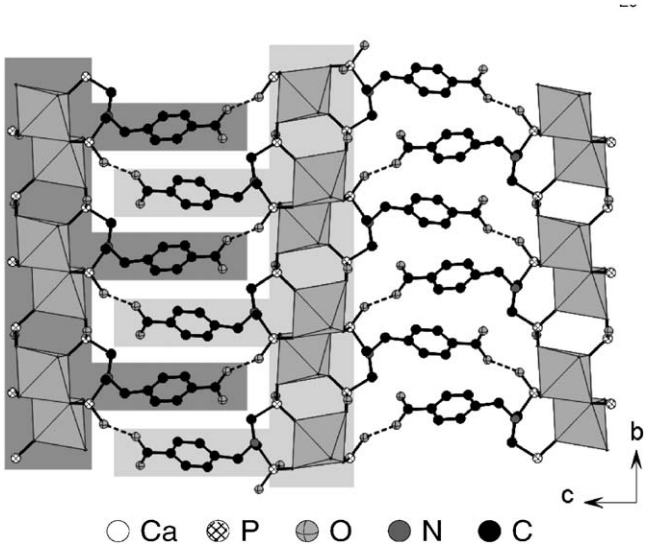

Fig. 10. Zipper-like connection of adjacent Ca-phosphonate layers in $Ca[H(O_3PCH_2)_2NH\text{-}CH_2C_6H_4\text{-}COOH]\cdot H_2O$ (**2**).

zwitterion, one Ca^{2+} ion on a special position, and two water molecules. The Ca^{2+} ions are octahedrally coordinated by four oxygen atoms of the phosphonate groups and two water molecules (Fig. S11). The Ca–O distances (2.280(2)–2.331(2) Å) are comparable to those found in the title compound **2** (2.303 (2)–2.442 (2) Å). Only one oxygen atom of each phosphonate group (O1 and O5) takes part in the coordination of Ca^{2+} ions. Thus, two adjacent CaO_6 octahedra are connected at a time by two iminobis(methylphosphonic acid)-units and one-dimensional chains of rings of isolated octahedra along the *b*-axis are formed (Fig. 11). These chains are further stabilized and connected along the *c*-axis by intensive hydrogen bonding. Thus, the CaO_6 are arranged in a layer parallel to the *b*,*c*-plane (Fig. 12). A view along the *b*-axis shows that the organic units are again arranged in a zipper-like fashion and point to adjacent layers. In contrast to the other compounds, the carboxylic acid unit can form two hydrogen bonds, connecting two neighboring chains of CaO_6 octahedra (Fig. 13). Fig. S7 and Table S5 in the Supplementary Material show all hydrogen bonds formed by the organic unit.

4.2. IR spectroscopy

All four title compounds were studied by IR spectroscopy (Fig. 14). In the following only bands related to the

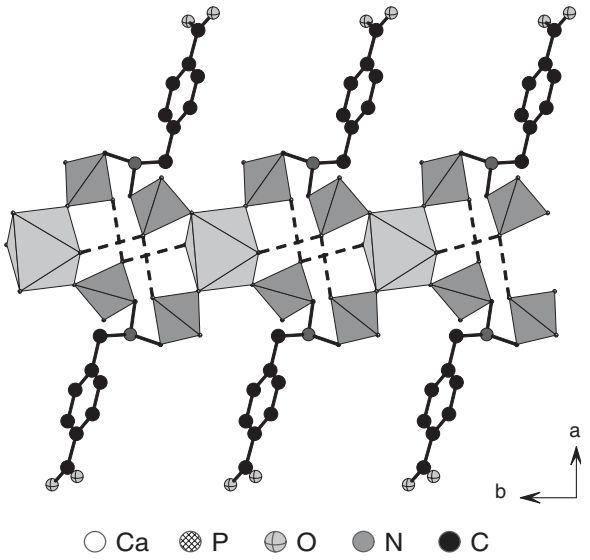

Fig. 11. One-dimensional chain of CaO_6 octahedra along the *b*-axis as observed in $Ca[(HO_3PCH_2)_2NH\text{-}CH_2C_6H_4\text{-}COOH]_2 \cdot 4H_2O$ (**3**). CaO_6 octahedra are shaded in light gray and PO_3C tetrahedra are shaded in dark gray. Hydrogen bonds are presented in dashed lines.

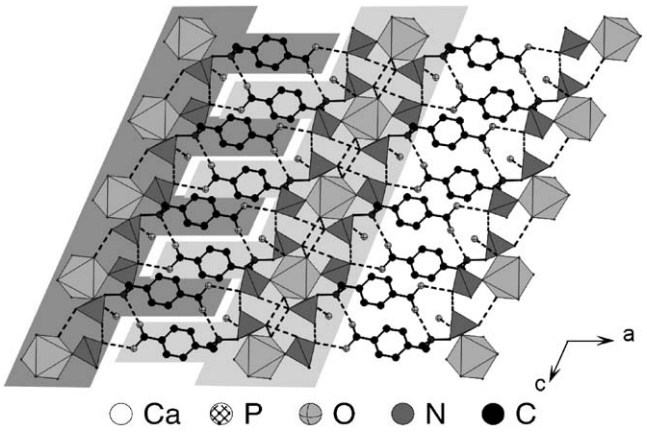

Fig. 13. The organic units are arranged in a zipper-like fashion and point to adjacent layers as observed in $Ca[(HO_3PCH_2)_2NH\text{-}CH_2C_6H_4\text{-}COOH]_2 \cdot 4H_2O$ (**3**). CaO_6 octahedra are shaded in light gray and PO_3C tetrahedra are shaded in dark gray.

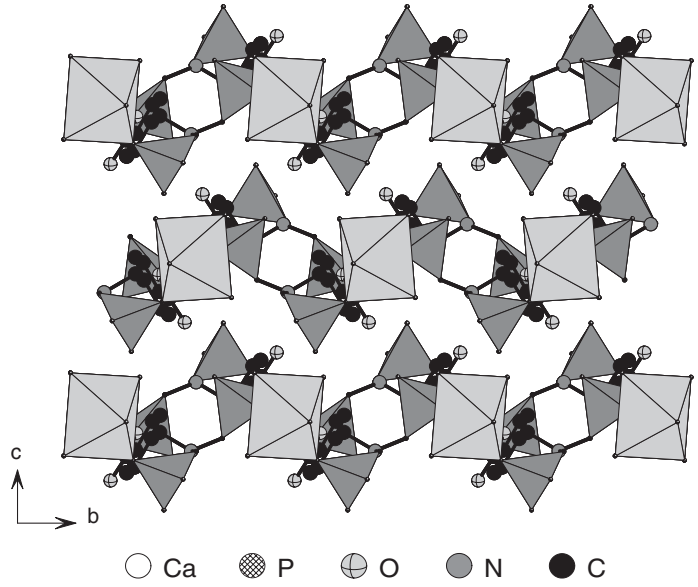

Fig. 12. The CaO_6 octahedra are arranged in the *b*,*c*-plane as observed in $Ca[(HO_3PCH_2)_2NH\text{-}CH_2C_6H_4\text{-}COOH]_2 \cdot 4H_2O$ (**3**). CaO_6 octahedra are shaded in light gray and PO_3C tetrahedra are shaded in dark gray.

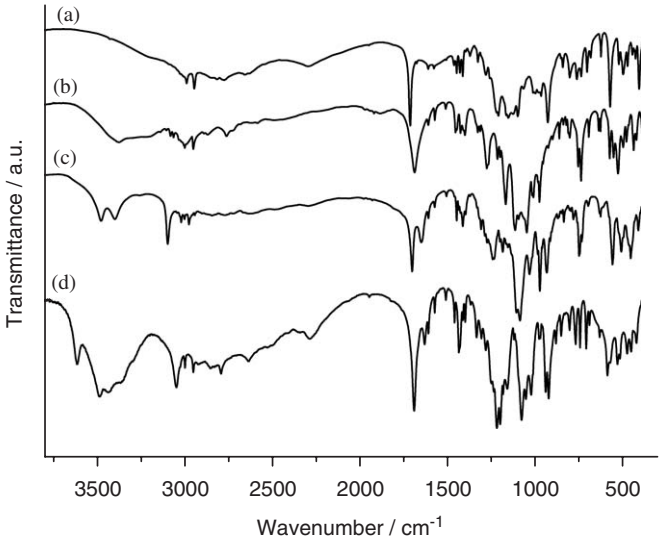

Fig. 14. IR-spectra for (a) $H(HO_3PCH_2)_2NH\text{-}CH_2C_6H_4\text{-}COOH$ (**H_5L**), (b) $Sm[(O_3PCH_2)_2NH\text{-}CH_2C_6H_4\text{-}COOH]\cdot H_2O$ (**1**), (c) $Ca[H(O_3PCH_2)_2NH\text{-}CH_2C_6H_4\text{-}COOH]\cdot H_2O$ (**2**), and (d) $Ca[(HO_3PCH_2)_2NH\text{-}CH_2C_6H_4\text{-}COOH]_2\cdot 4H_2O$.

presence of water molecules, hydrogen bonding, and carboxylic acid groups are discussed in detail, since they give valuable structural information. The IR-spectra of all compounds exhibit typical bands in the region between 1250 and 980 cm^{-1} that are due to the P–C and P–O stretching vibrations of the tetrahedral CPO_3-group.

In the IR-spectrum of $H(HO_3PCH_2)_2NH\text{-}CH_2C_6H_4\text{-}COOH$ (**H_5L**) the absence of bands due the vibrations of water molecules is in accordance with crystallographic results. Several broad bands of low intensity in the region between 2900 and 2200 cm^{-1} are due to O–H stretching vibrations involved in H-bonding of the hydrogen phosphonate groups [19]. The band corresponding to the C=O stretching vibration of the carboxylic acid group is located at 1717 cm^{-1}, which is a typical value for carboxylic groups involved in hydrogen bonding.

In accordance with the crystallographic results that the water molecules in $Sm[(O_3PCH_2)_2NH\text{-}CH_2C_6H_4\text{-}COOH]\cdot H_2O$ (**1**) are involved in a complex hydrogen-bonding scheme, a broad band at 3373 cm^{-1} is present. The corresponding deformation band appears at 1615 cm^{-1}. Bands in the region from 3079 to 2950 cm^{-1} are due to aromatic and aliphatic C–H stretching vibrations. Several broad bands from 2800 to 2500 cm^{-1} may be assigned to O–H stretching vibrations of the carboxylic acid groups involved in hydrogen bonding. The C=O stretching vibration of the carboxylic acid group appears as a rather broad band at 1693 cm^{-1}.

The presence of two broad bands at 3475 and 3396 cm^{-1} in the IR spectrum of $Ca[H(O_3PCH_2)_2NH\text{-}CH_2C_6H_4\text{-}COOH]\cdot H_2O$ (**2**) clearly indicates that hydrogen-bonded water molecules are part of the structure. The corresponding deformation band appears at 1655 cm^{-1}. The aromatic and aliphatic C–H stretching vibrations result in a set of sharp bands in the region from 3096 to 2975 cm^{-1}. Several broad bands of low intensity in the region from 2845 to 2200 cm^{-1} are due to O–H stretching vibrations of the hydrogen phosphonate and the carboxylic acid groups involved in hydrogen bonding. The C=O stretching vibration of the carboxylic acid group can be assigned to the sharp band at 1706 cm^{-1}. The higher frequency in comparison to the C=O stretching vibration in compound **1** is in agreement with the shorter C=O bond distance (1.199(3) and 1.217(7) Å, respectively).

The sharp and well-defined band at 3613 cm^{-1} in the IR spectrum of $Ca[(HO_3PCH_2)_2NH\text{-}CH_2C_6H_4\text{-}COOH]_2\cdot 4H_2O$ (**3**) can be assigned to O–H stretching vibration of one of the water molecules with the hydrogen atoms not being involved in hydrogen bonding. This is in accordance with crystallographic results. The broad band from 3483 to 3358 cm^{-1} clearly indicates the presence of the other water molecules that are involved in hydrogen bonding. The C–H stretching vibrations of the aromatic and aliphatic groups can be assigned to the set of sharp bands in the region between 3047 and 2950 cm^{-1}. Several bands in the region from 2854 to 2291 cm^{-1} indicate an extensive scheme of hydrogen bonding. The sharp band at 1696 cm^{-1} is due to the C=O stretching vibration of the carboxylic acid group.

4.3. Thermal properties

The thermal properties of the title compounds were studied using TG analysis (Fig. 15). Additionally, $Sm[(O_3PCH_2)_2NH\text{-}CH_2C_6H_4\text{-}COOH]\cdot H_2O$ (**1**) was characterized using temperature-dependent X-ray powder diffraction (Fig. 16).

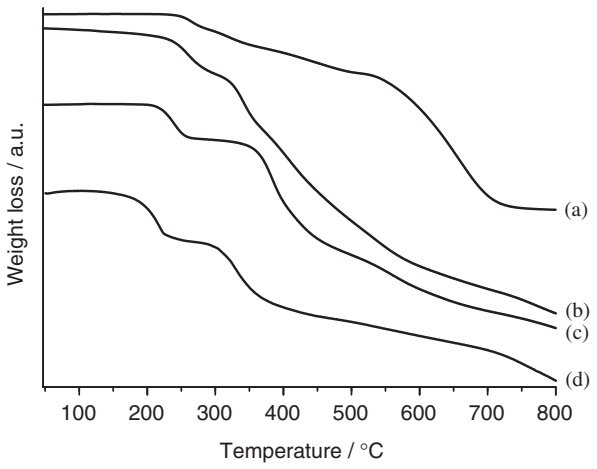

Fig. 15. TG curves for (a) $H(HO_3PCH_2)_2NH\text{-}CH_2C_6H_4\text{-}COOH$ (**H_5L**), (b) $Sm[(O_3PCH_2)_2NH\text{-}CH_2C_6H_4\text{-}COOH]\cdot H_2O$ (**1**), (c) $Ca[H(O_3PCH_2)_2NH\text{-}CH_2C_6H_4\text{-}COOH]\cdot H_2O$ (**2**), and (d) $Ca[HO_3PCH_2)_2NH\text{-}CH_2C_6H_4\text{-}COOH]_2\cdot 4H_2O$.

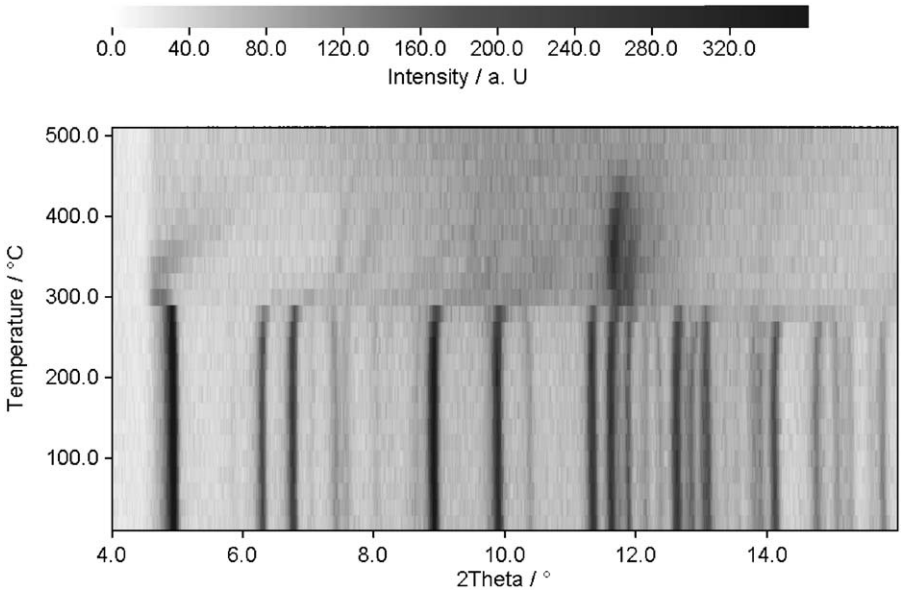

Fig. 16. Temperature-dependent X-ray diffraction of $Sm[(O_3PCH_2)_2NH\text{-}CH_2C_6H_4\text{-}COOH]\cdot H_2O$ (**1**).

In the TG diagram of H_5L up to 235 °C no weight loss is observed. The decomposition of the compound due to condensation of the phosphonic and carboxylic acid groups and the pyrolysis upon further heating proceeds in two major steps. Up to 520 °C a weight loss of 28% is observed followed by weight loss of 63%, which is completed at 750 °C.

The TG diagram of $Sm[(O_3PCH_2)_2NH\text{-}CH_2C_6H_4\text{-}COOH]\cdot H_2O$ (**1**) shows no significant weight loss up to 210 °C. From 210 to 300 a weight loss of 3.7%, which corresponds to the release of the lattice water molecule (calcd. 3.6%). With increasing temperature a steady loss is observed. Thus, the departure of water, which is completed at 290 °C according to TG measurement, leads to a change in the structure. A new, unknown crystalline phase appears from 290 °C on and is present to 480 °C. Beyond 480 °C the sample is X-ray amorphous.

According to TG measurements, $Ca[H(O_3PCH_2)_2NH\text{-}CH_2C_6H_4\text{-}COOH]\cdot H_2O$ (**2**) is stable up to 200 °C (Fig. 15). Thus, no weight loss is observed. From 200 to 290 °C a one step loss of 5.7% occurs. The calculated value for the release of one lattice water molecule is 4.6% indicating that in this step condensation of hydrogen phosphonate and carboxylic acid groups takes place. Upon further heating a continuous weight loss due to decomposition of the sample is observed.

In $Ca[(HO_3PCH_2)_2NH\text{-}CH_2C_6H_4\text{-}COOH]_2\cdot 4H_2O$ (**3**) a single-step weight loss is observed from 120 to 280 °C. The value 11.3% (calcd. 11.4%) corresponds to the departure of five water molecules per formula unit (Fig. 15). Thus, not only the lattice water molecules are released but also water from the condensation of hydrogen phosphonate and carboxylic acid groups resulting in a collapse of the structure. Upon further heating a continuous weight loss due to further condensation and pyrolysis of the organic part is observed.

5. Conclusions

Single-crystal structure determination of the organic building block $H(HO_3PCH_2)_2NH\text{-}CH_2C_6H_4\text{-}COOH$ revealed that the crystal structure is composed of zwitterions formed by the protonation of the nitrogen atom. This compound was successfully employed in the synthesis of new metal phosphonates and in all cases the protonation of the nitrogen in metal phosphonates was observed. This is in accordance with the work of other groups employing iminobis(methylphosphonic acid) and its derivatives [20–22]. Comparing the metal phosphonates, $Sm[(O_3PCH_2)_2NH\text{-}CH_2C_6H_4\text{-}COOH]\cdot H_2O$ (**1**), $Ca[H(O_3PCH_2)_2NH\text{-}CH_2C_6H_4\text{-}COOH]\cdot H_2O$ (**2**), and $Ca[(HO_3PCH_2)_2NH\text{-}CH_2C_6H_4\text{-}COOH]_2\cdot 4H_2O$ (**3**), all exhibit a similar zipper-like arrangement of the rigid phenyl carboxylic acid (Fig. 17). The structures are stabilized through the formation of H-bonding between the carboxylic acid group and a phosphonate or the amine group (C-OH···O=P, C-OH···N, respectively). But, due to different oxidation states and ionic radii of the cations as well as different synthesis temperatures a variation in the dimensionality of the inorganic building units are observed. In the case of Sm^{3+} ions (coordination number: 8; ionic radius: 1.219 Å [23]), the higher ionic charge in comparison to Ca^{2+} permits the complete deprotonation of the phosphonic acid groups, which leads to a higher dimensionality of the network. Thus, chains of SmO_8 polyhedra are formed, which are further connected via phosphonate groups to form a samarium phosphonate layer. At the same reaction temperature (150 °C), $Ca[H(O_3PCH_2)_2NH\text{-}CH_2C_6H_4\text{-}COOH]\cdot H_2O$ was

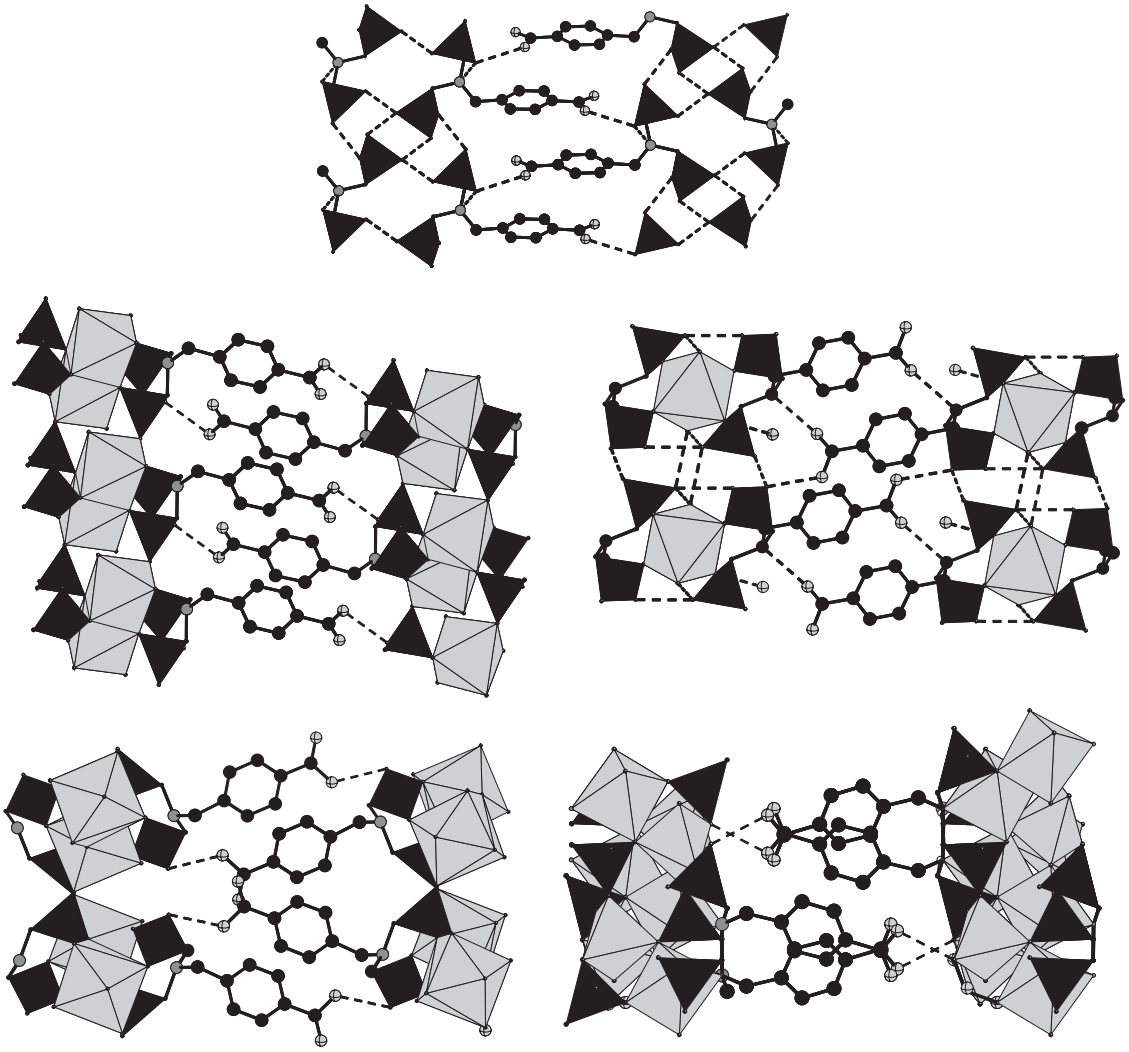

Fig. 17. Zipper-like arrangement of the rigid phenyl carboxylic acid moiety in $H(O_3PCH_2)_2NH\text{-}CH_2C_6H_4\text{-}COOH$ (**H_5L**) (top), $Ca[H(O_3PCH_2)_2NH\text{-}CH_2C_6H_4\text{-}COOH]\cdot H_2O$ (**2**) (middle left), $Ca[(HO_3PCH_2)_2NH\text{-}CH_2C_6H_4\text{-}COOH]_2\cdot 4H_2O$ (**3**) (middle right), $Sm[(O_3PCH_2)_2NH\text{-}CH_2C_6H_4\text{-}COOH]\cdot H_2O$ (**1**) (bottom left), and $Co_2[(O_3PCH_2)_2N\text{-}CH_2C_6H_4\text{-}COOH]\cdot H_2O$ (bottom, right) [9]. Metal-oxygen polyhedra are shaded in light gray and PO_3C tetrahedra are shaded in dark gray.

formed (ionic radius of six fold coordinated Ca^{2+}: 1.14 Å [22]). In this compound one phosphonic acid group remains mono-protonated. The metal-oxygen building units are of lower dimensionality compared to those in the Sm-compound. Ca_2O_6 units are present, which are connected via phosphonate groups and thus, a Ca-phosphonate layer further stabilized by hydrogen bonding is formed. In the case of $Ca[(HO_3PCH_2)_2NH\text{-}CH_2C_6H_4\text{-}COOH]_2\cdot 4H_2O$, which is formed at lower temperatures (100 °C), both phosphonic acid groups remain mono-protonated and the dimensionality of the inorganic building units is therefore even lower (isolated CaO_6 octahedra). In addition, more water molecules are incorporated into the structure. The fact that with elevated temperature for identical initial compositions the formed structures exhibit a higher grade of condensation and less water molecules are found to be incorporated into the structure is also observed in a recent systematic investigation on the formation of Cobalt succinates under hydrothermal conditions [24].

The phosphonocarboxylic acid, H_5L, has shown to be a versatile and flexible starting material in the synthesis of new metal phosphonates. In addition to the recently obtained open-framework compound $Ba_3[O_3PCH_2NH_2CH_2PO_3]_2\cdot 7H_2O$ [8], which is a reaction product of the in situ decomposition of H_5L and several new cobalt carboxy-phosphonates [9], we were able to synthesize three new metal carboxy-phosphonates, employing Sm^{3+} and Ca^{2+}. In all observed structures, derived from $H(HO_3PCH_2)_2NH\text{-}CH_2C_6H_4\text{-}COOH$, the carboxylic acid group remained protonated. A carboxylate group involved in the coordination of metal ions should lead to a higher dimensionality that is mandatory for an open framework structure. In order to study this effect reactions under more basic conditions are currently performed.

Supplementary material: CCDC 285963 ($H(HO_3PCH_2)_2NH\text{-}CH_2C_6H_4\text{-}COOH$), CCDC 285964 ($Sm[(O_3PCH_2)_2NH\text{-}CH_2C_6H_4COOH]\cdot H_2O$ (**1**)), CCDC 285965 ($Ca[H(O_3PCH_2)_2NH\text{-}CH_2C_6H_4\text{-}COOH]\cdot H_2O$ (**2**)), and CCDC 285966 ($Ca[(HO_3PCH_2)_2NH\text{-}CH_2C_6H_4\text{-}COOH]_2\cdot 4H_2O$ (**3**)) contain the supplementary crystallographic data for this paper. These data can be obtained free of charge from the Cambridge Crystallographic Data Centre via www.ccdc.cam.ac.uk/data_request/cif. In addition, the molar ratios $xSm{:}yH_5L{:}z$NaOH in the high-throughput experiment and the figures of the asymmetric units of ($H(HO_3PCH_2)_2NH\text{-}CH_2C_6H_4\text{-}COOH$), **1**, **2**, and **3**, as well as the tables describing the hydrogen bonding in the latter compounds (Tables S2–S5) are given. Furthermore, the experimental and theoretical XRD powder patterns of compounds **1–3** are presented.

Acknowledgments

The authors thank Dr. P. Mayer for the acquisition of the single-crystal data of $(HO_3PCH_2)_2NH\text{-}CH_2C_6H_4\text{-}COOH$, **1**, and **2**, and Priv.-Doz. Dr. Christian Näther for the acquisition of the single-crystal data of **3**.

Appendix A. Supplementary materials

Supplementary data associated with this article can be found in the online version at doi:10.1016/j.jssc.2005.10.008.

References

[1] A.K. Cheetham, G. Férey, T. Loiseau, Angew. Chem. Int. Ed. 38 (1999) 3268.
[2] M. Eddaoudi, J. Kim, N. Rosi, D. Vodak, J. Wachter, M. O'Keeffe, O.M. Yaghi, Science 295 (2002) 469.
[3] K. Maeda, Microporous Mesoporous Mater. 73 (2004) 47.
[4] T. Bein, Angew. Chem. Int. Ed. 38 (1999) 323.
[5] K. Choi, D. Gardner, N. Hilbrandt, T. Bein, Angew. Chem. Int. Ed. 38 (1999) 2891.
[6] N. Stock, T. Bein, Angew. Chem. 116 (2004) 767;
N. Stock, T. Bein, Angew. Chem. Int. Ed. 43 (2004) 749.
[7] N. Stock, T. Bein, J. Mater. Chem. 15 (2005) 1384.
[8] S. Bauer, H. Müller, T. Bein, N. Stock, Inorg. Chem., in press, doi:10.1021/ic050935m.
[9] S. Bauer, T. Bein, N. Stock, Inorg. Chem. 44 (2005) 5882.
[10] N. Stock, M. Rauscher, T. Bein, J. Solid State Chem. 177 (2004) 642.
[11] N. Stock, A. Stoll, T. Bein, Microporous Mesoporous Mater. 69 (2004) 65.
[12] J.-L. Song, A.V. Prosvirin, H.-H. Zhao, J.-G. Mao, Eur. J. Inorg. Chem. (2004) 3706.
[13] J.-L. Song, J.-G. Mao, J. Mol. Struct. 740 (2005) 181.
[14] K. Moedritzer, R.R. Irani, J. Org. Chem. 31 (1966) 1603.
[15] N. Stock, T. Bein, Solid State Sci. 5 (2003) 1207.
[16] XRED, data reduction and absorption correction program version 1.09 for Windows, Stoe & Cie GmbH, Darmstadt, 1997.
[17] G.M. Sheldrick, SHELXTL-PLUS Crystallographic System, Siemens, Analytical X-ray Instruments Inc., Madison, WI, 1992.
[18] G.A. Jeffrey, in: D.G. Truhlar (Ed.), Topics in Physical Chemistry: An Introduction to Hydrogen Bonding, Oxford University Press, New York, 1997.
[19] L.J. Bellamy, Infrared Spectra of Complex Molecules, Wiley, New York, 1958 (Chapter 18).
[20] J.-L. Song, J.-G. Mao, Y.-Q. Sun, H.-Y. Zeng, R.K. Kremer, A. Clearfield, J. Solid State Chem. 177 (2004) 633.
[21] R. Vivani, U. Costantino, M. Nocchetti, J. Mater. Chem. 12 (2002) 3254.
[22] A. Cabeza, S. Bruque, A. Guagliardi, M.A.G. Aranda, J. Solid State Chem. 160 (2001) 278.
[23] R.D. Shannon, C.T. Prewitt, Acta Crystallogr. B25 (1969) 925.
[24] P.M. Forster, N. Stock, A.K. Cheetham, Angew. Chem. Int. Ed. 2005, in press, doi:10.1002/ange.200501766.